Journal of Materials Chemistry A

Thermodynamic stability and correlation with synthesis conditions, structure and phase transformations in orthorhombic and monoclinic $Li_2M(SO_4)_2$ (M = Mn, Fe, Co, Ni) polymorphs

Journal:	*Journal of Materials Chemistry A*
Manuscript ID:	TA-ART-09-2014-005066.R1
Article Type:	Paper
Date Submitted by the Author:	18-Nov-2014

Complete List of Authors:	Radha, A V; University of California Davis, NEAT ORU Lander, Laura; College de France, Rousse, Gwenaëlle; Institut de Minéralogie et de Physique des Milieux Condensés, Chemistry Tarascon, Jean-Marie; College de France, Navrotsky, Alexandra; University of California at Davis, NEAT ORU and Thermochemistry Facility

Table of contents entry / Graphical Abstract

Thermodynamic stability and correlation with synthesis conditions, structure and phase transformations in orthorhombic and monoclinic $Li_2M(SO_4)_2$ (M = Mn, Fe, Co, Ni) polymorphs A.V. Radha, L. Lander, G. Rousse, J.M. Tarascon and A. Navrotsky Calorimetric studies demonstrate that higher symmetry orthorhombic $Li_2M(SO_4)_2$ (M = Co, Fe) have lower energetic stability than the corresponding monoclinic phases. However, the positive enthalpies of formation for both monoclinic and orthorhombic polymorphs indicate that their formation is entropy driven, possibly due to vibrational/rotational disorder of the SO_4 tetrahedra.	**$Li_2M(SO_4)_2$ polymorphs** 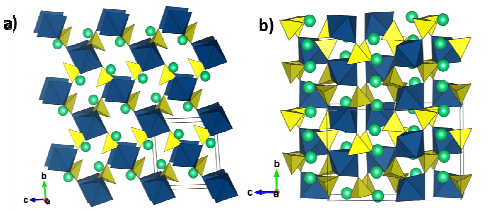 **Monoclinic** **Orthorhombic**

Thermodynamic stability and correlation with synthesis conditions, structure and phase transformations in orthorhombic and monoclinic $Li_2M(SO_4)_2$ (M = Mn, Fe, Co, Ni) polymorphs

A.V. Radha,[a] L. Lander,[b] G. Rousse[b], J.M. Tarascon[b] and A. Navrotsky [a]

[a]Peter A. Rock Thermochemistry Laboratory and NEAT ORU (Nanomaterials in the Environment, Agriculture and Technology Organized Research Unit), University of California, One Shields Avenue, Davis, CA 95616, USA.

[b]FRE 3677 Collège de France, 11 place Marcelin Berthelot, 75231 Paris Cedex 05, France

Abstract:

Rational design and development of new Li-polyanion battery materials by exercising synthetic control have led to a new class of $Li_2M(SO_4)_2$ compounds in monoclinic (M = Mn, Fe, Co) and orthorhombic (M = Fe, Co, Ni) polymorphic forms, using solid state (ceramic) and ball milling methods respectively. The enthalpies of formation from binary sulfates determined using isothermal acid solution calorimetry are positive, and show decrease in energetic metastability with increase in ionic radius for both monoclinic and orthorhombic (except for Ni) polymorphs. The higher symmetry orthorhombic polymorphs with Fe and Co are energetically less stable than the corresponding monoclinic polymorphs. The vibrational/rotational disorder of the SO_4 tetrahedra is identified as the most likely cause of the entropy term ($T\Delta S$) of the free energy to overcome the positive enthalpy of formation in monoclinic and orthorhombic phases. Driven by thermodynamic metastability, the orthorhombic $Li_2M(SO_4)_2$ (M = Fe, Co) polymorphs transform irreversibly into the monoclinic phase on heat treatment. Orthorhombic $Li_2Ni(SO_4)_2$, formed by a ceramic route is thermodynamically stable and does not transform to the monoclinic phase on heating. The formation of metastable orthorhombic samples by ball milling is

consistent with earlier thermodynamic studies on other Li-hydroxy/fluorosulfate systems, for which metastable tavorite polymorphs could be formed only by mild chemical synthetic approaches. This work demonstrates that the entropy term can play a key role for the synthesis, stability and phase transformation among polymorphs of Li-polyanionic compounds.

Keywords: Li-ion battery cathodes, monoclinic and orthorhombic $Li_2M(SO_4)_2$ polymorphs, calorimetry, energetic stability

1. Introduction

New challenges of developing high performance energy storage devices for electric vehicles and grid storage technologies have led to the emergence of lithium containing polyanion framework compounds as candidates for next generation cathode materials.[1-9] The possibility of tuning open-circuit voltage of these materials by enhanced inductive effects through reduction of the metal-anion bond covalency using different polyanions has produced lithium framework compounds such as iron/manganese/cobalt/nickel phosphates,[1, 10-15] vanadium/fluorophosphates,[16-18] pyrophosphates,[19, 20] silicates,[21-23] fluorosulfates,[24-27] hydroxysulfates, [28-30] vanadates,[31, 32] molybdates[33-35] and borates.[36, 37] Naturally abundant Fe and Mn based systems have generated interest due to their low cost, low toxicity and high gravimetric capacity. However, implementation of these polyanionic materials for practical application needs better control over their syntheses, and chemical composition as well as understanding of their structure, polymorphism and stability under battery operating conditions.

Calorimetric studies of energetic trends in fluorosulfate and hydroxysulfate based polyanionic Li-battery materials have already provided insights into thermodynamic influence on structure, phase selection (polymorphism) and electrochemical behavior.[38, 39] For instance, Li-fluorosulfates exists in two

different structures and exhibits redox potentials of 3.9 V and 3.6 V vs. Li^+/Li for triplite and tavorite $LiFeSO_4F$ polymorphs. Calorimetric studies show that at ambient temperature both polymorphs are energetically similar, which makes low temperature synthesis and isolation of single phase material difficult.[38] However, entropy favors the disordered triplite and this observation motivated subsequent synthesis of pure triplite phase by ball milling and spark plasma sintering (SPS) techniques, which considerably increase disorder by creating defects.[40] In layered lithium hydroxysulfates $LiMSO_4OH$ (*M* = Co, Fe and Mn), thermodynamic stability and redox potential decrease with increase in ionic radius reflecting weaker M-O bonds and structural distortions.[29, 39] This provides further evidence for possible correlation between thermodynamic stability, redox potential and structural distortions as indicated by lowering of sulfate bonding symmetry from C_{3v} to C_{2v}.

Based on this knowledge, recently ionothermal, ball milling and low temperature solid state synthetic approaches have provided synthetic control over polymorphism in development of new Li-polyanionic battery materials.[41-48] A new class of Li-metal sulfate compounds, $Li_2M(SO_4)_2$ has been obtained in monoclinic marinite $Li_2M(SO_4)_2$ (*M* = Mg, Mn, Fe, Co) and orthorhombic $Li_2M(SO_4)_2$ (M = Fe, Co, Ni, Zn) polymorphic forms using solid state (ceramic) processing and ball milling, respectively.[42, 43] Among these, only $Li_2Fe(SO_4)_2$ in both monoclinic marinite (3.83 vs Li^+/Li^0) and orthorhombic (3.73 and 3.85 V vs Li^+/Li^0 with a two-step redox process) polymorphs is electrochemically active, while phases containing Mn, Ni and Co are inactive.[42] However, these polymorphs exhibit interesting phase transformation behavior, monoclinic phases except $Li_2Mn(SO_4)_2$ transform into orthorhombic phases on mechanical milling, while orthorhombic phases except $Li_2Ni(SO_4)_2$ transform to monoclinic phases on heating.[42] Furthermore, single phase orthorhombic $Li_2Mn(SO_4)_2$ and monoclinic $Li_2Ni(SO_4)_2$ could not be obtained by any synthetic method, suggesting that larger cations favor the monoclinic phase, and smaller cations the orthorhombic.

In this work, we determined the enthalpies of formation of $Li_2M(SO_4)_2$ (M = Mn, Fe, Co and Ni) phases in order to understand thermodynamic driving forces behind phase stability and transformation behavior in this new class of materials. The calorimetric measurements were performed using isothermal acid solution calorimetry in 5 M HCl at 25 °C on three monoclinic marinite $Li_2M(SO_4)_2$ (M = Mn, Fe, Co) and three orthorhombic $Li_2M(SO_4)_2$ (M = Fe, Co, Ni) samples.

2. Experimental Methods

2.1 Syntheses

Orthorhombic phases: Stoichiometric amounts of anhydrous MSO_4 (M= Co, Fe) and Li_2SO_4 were ball-milled for several hours with a Retsch PM100 planetary mill. For $Li_2Co(SO_4)_2$ the starting materials were ball-milled for 10 hours (divided into 30 min steps with 15 min pauses) under air atmosphere and for $Li_2Fe(SO_4)_2$ 5 hours (divided into 30 min steps with 15 min pauses) under argon atmosphere to avoid oxidation of Fe^{2+} to Fe^{3+}. $Li_2Ni(SO_4)_2$ was prepared by a ceramic route, which includes ball milling of stoichiometric ratios of Li_2SO_4 and $NiSO_4$ for 20 min using a Spex 8000 vibratory mill, pressing the resulting mixture into a pellet and heating at 500 °C for 24 hours.

Monoclinic phases: $Li_2M(SO_4)_2$ (M = Mn, Fe and Co) monoclinic phases were synthesized via a ceramic process that involved two key steps: *(i)* stoichiometric ratios of the sulfate precursors Li_2SO_4 and MSO_4 were ball-milled for 20 min using a Spex 8000 vibratory mill, and *(ii)* the resulting mixtures were pressed into pellets and annealed at different temperatures for different times, depending on the nature of the metal. Given the propensity of Fe^{2+} to oxidize, the second step was conducted in a silica tube sealed under vacuum at 320 °C for 72 hours. The monoclinic cobalt phase was obtained through heat treatment at 400 °C overnight and the manganese phase by heating for 4 days at 350 °C.

Sample syntheses were done at the College de France, and the samples were then shipped under Ar atmosphere in sealed screw capped vials to UC Davis for further characterization and calorimetry. All samples were stored and prepared for X-ray powder diffraction (XRD), TG-DSC, FTIR, and calorimetric measurements in a hard wall nitrogen-filled glovebox with oxygen content < 5 ppm (tested with burning of a bare light bulb filament).

2.2 X-ray Powder diffraction (XRD)

A Bruker D8 Advance diffractometer with a Cu-Kα radiation source (λ_1 =1.5405Å, λ_2 = 1.5443Å) and a Lynxeye XE detector was used to collect the powder XRD patterns of the as-prepared $Li_2M(SO_4)_2$ (*M*= Mn, Fe, Co, Ni) phases. The XRD patterns were recorded for 1 h in the 2θ range of 10-55 ° with a step size of 0.015 °. The Rietveld refinement of monoclinic $Li_2Fe(SO_4)_2$ shows the presence of about 2.75 wt % $FeSO_4$ while all the other samples were single phase.

2.3 Solid-state infrared (IR) spectroscopy

IR spectra of samples were collected with a Bruker Equinox 55 FTIR spectrometer (range 400-4000 cm^{-1}) with Opus software. A pelletized sample was prepared from the ground mixture of sample and KBr in 1:100 w/w ratio inside the nitrogen glovebox using a pellet die and then loaded into the spectrometer within 90 seconds after removal from the glovebox. A background spectrum collected with a pure KBr pellet was subtracted from each sample spectrum to remove the effects of water and CO_2 vapors present inside the sample chamber. The O-H modes observed around 3600 cm^{-1} (a very broad) and 1600 cm^{-1} in the FTIR spectra could have arisen due to adsorption of water on exposure to air while loading the sample for spectroscopic measurement.

2.4 Thermogravimetric analysis (TGA)

A Netzsch STA 449 system (Selb, Germany) was used to run TGA of all samples. The sample was loaded into an alumina crucible inside a nitrogen glove box and then transferred to the STA 449

system within 1-2 min. The sample was heated at 10 °C/min to 700 °C with argon flow. A baseline collected with an empty crucible was subtracted for buoyancy correction.

2.5 Isothermal Acid Solution Calorimetry

Both CSC 4400 isothermal (with IMC data acquisition software) and Hart Scientific (with Labview software) microcalorimeters with mechanical stirring were used to measure the enthalpies of dissolution of the samples and reagents at 25 °C. Calorimeters were calibrated with KCl (NIST standard reference material) by dissolving 15 mg pellets in 25 g of water at 25 °C. The solution enthalpy of this reference concentration (0.008 mol/kg) deduced from the literature and enthalpy of dilution measurements were used to arrive at the calorimeter calibration factor. In a typical calorimetric run, 4-7 mg of sample was pressed into a pellet inside a nitrogen glove box and then dropped into 25 g of 5M HCl placed in the sample chamber of the calorimeter with minimum exposure to air (≤ 1 min). The sample dissolution causes the heat flow due to temperature difference and is recorded as a calorimetric signal. The integrated area under the recorded microwatt signal from a linear baseline corresponds to total heat effects, which on conversion into joules with KCl calibration corresponds to the enthalpy of sample dissolution (ΔH_{solun}). An appropriate thermochemical cycle based on Hess' law was used to calculate the enthalpy of formation.

3. Results and Discussion

Figure 1 shows the powder XRD patterns of the $Li_2M(SO_4)_2$ samples of monoclinic (*M* = Mn, Fe and Co) and orthorhombic (*M* = Fe, Co and Ni) structures. The orthorhombic structure for $Li_2M(SO_4)_2$ (*M* = Fe and Co) phases (space group *Pbca*) was reported by Lander et al[42] (using Rietveld refinements of XRD patterns with the orthorhombic $Li_2Ni(SO_4)_2$ structure model proposed by Isasi et al.[49]). The structures of monoclinic phases (space group $P2_1/c$) were reported earlier by Reynaud et al.[41,

[45] Comparing the XRD patterns of the various members of the two polymorph families, one can see that for both monoclinic and orthorhombic phases, the peak positions in XRD patterns move to slightly higher 2θ values with decrease in ionic radius of cations. This trend reflects the decrease of lattice parameters and resulting unit cell volumes with decreasing ionic radius.[42, 45]

Figure 2 shows representative crystal structures of monoclinic and orthorhombic $Li_2M(SO_4)_2$ phases. Both structures have three dimensional frameworks made up of isolated MO_6 octahedra that are only connected through the oxygen atoms to six corner sharing SO_4 tetrahedra, while each SO_4 group is connected to three corner sharing MO_6 octahedra. The main difference between the two polymorphs is the way in which the SO_4 and MO_6 polyhedra are interconnected as shown in Figure 2, which results in shorter *M*-*M* distances and a higher density/lower volume for the orthorhombic phases.[19] For the tavorite-triplite system, polymorphism is associated with long range structural disorder (statistical occupancy of Li and *M* cations on the same crystallographic site). However there is no positional disorder in the present case. The crystal structure data for monoclinic and orthorhombic $Li_2M(SO_4)_2$ show the existence of different atomic positions for Li, *M* and sulfate group atoms.[41-45] In the monoclinic structure, *M* occupies the *2a* Wyckoff site, two Li cations occupy the single *4e* site, and two SO_4 anion groups occupy the same set of five *4e* sites having different co-ordinates. In orthorhombic structure, *M* occupies the *8c* site, two Li cations occupy two separate *8c* sites with different coordinates and 10 atoms from two SO_4 groups occupy ten different *8c* sites. This suggests the existence of Li in two different environments and similarly, separate sites for each of two sulfate groups implies the crystallographically distinct sulfate groups having different orientations in the orthorhombic structure. Thus there is no positional disorder in the orthorhombic phase.

The FTIR spectra in Figure 3 illustrate the different sulfate binding symmetries in monoclinic and orthorhombic samples. In general, the sulfate anion displays four vibrational modes corresponding

to symmetric stretch (ν_1 ~ 980 cm^{-1}), asymmetric stretch (ν_3 ~ 1100 cm^{-1}), symmetric bend (ν_2 ~ 450 cm^{-1}), and asymmetric bend (ν_4 ~ 610 cm^{-1}).[50] For a free sulfate anion in T_d symmetry, only triply degenerate ν_3 and ν_4 modes are IR active. In solids, the distortions in sulfate polyhedra on bonding with cations lowers the symmetry, leading to removal of degeneracy, appearance of all other modes of vibrations as well as shifts in positions of absorption bands.[51-53] The splitting of ν_3 (1115 and 1185 cm^{-1}) and ν_4 (620 and 643 cm^{-1}) absorption bands into doublets and the presence of IR active ν_1 (1016 cm^{-1}) band in the FTIR spectra (Fig 3a) indicate the presence of sulfate in C_{3v} symmetry in monoclinic samples. In orthorhombic samples, the FTIR spectra show the presence of ν_3 (1109 and 1173 cm^{-1}) doublet and a very weak probably ν_1 (1000 cm^{-1}) absorption band for $Li_2M(SO_4)_2$ (M = Fe, Co), whereas these modes are poorly defined for $Li_2Ni(SO_4)_2$. However, the FTIR spectra of all orthorhombic samples show a broad ν_4 band with fine structures or quintuplet in 595 - 710 cm^{-1} range, which could arise due to presence of two distinct SO_4 groups and further decrease in sulfate symmetry.[51] This investigation into short range disorder by IR studies shows C_{3v} binding symmetry for monoclinic phases having a single set of atomic sites for both SO_4 groups, but lower C_1 symmetry for orthorhombic phases due to two crystallographically distinct types of SO_4 groups. These observations suggest the possibility of different types of local structural disorder in monoclinic and orthorhombic $Li_2M(SO_4)_2$ polymorphs. Nevertheless the origin of this disorder remains an open question. A possible other source of disorder could lie in the vibrations/rotations of SO_4 tetrahedra. Previous studies have revealed the feasibility of rotational disorder of SO_4/ClO_4^- tetrahedra for many sulfates and perchlorates, frequently referred to as a "paddle wheel" mechanism of motion of the SO_4/ClO_4 groups.[54-61]

The TGA curves of both monoclinic and orthorhombic samples show a continuous weight loss below 250 – 300 °C due to the presence of adsorbed water (see Table 1 for water contents). Despite all sample preparations being done in the glove box, the samples seem to have picked up adsorbed water,

probably due to exposure to air (for 30 - 60 sec) while loading them into the TGA/IR instrument and/or dropping them into the calorimeter. Water adsorption might also have occurred during sample transport between the two laboratory locations even though the samples were sealed in plastic bags. The samples were thoroughly checked for their reactivity towards water by leaving them overnight in ambient atmosphere. The XRD patterns of the aged samples were identical to those of pristine ones, implying unambiguously that the water adsorbed, if any, by samples is not structural water. Thus we believe that the water detected by TGA is surface water, consistent with the observed low temperature (~150 °C) water release.

The sulfate decomposition reactions occur at different temperatures for different cations. For Co and Mn, decomposition occurs around 700 °C, while the Fe based samples are thermally less stable and decompose around 500 °C, probably with oxidation of Fe^{2+} to Fe^{3+}.

Table 1 gives solution calorimetric data. The enthalpies of dissolution (ΔH_{solun}) in 5 M HCl at 25 °C range from -18.58 ± 0.34 to -37.54 ± 0.2 kJ/mol for monoclinic $Li_2M(SO_4)_2$ (M = Mn, Fe and Co) and -40.80 ± 0.40 to -49.00 ± 0.30 kJ/mol for orthorhombic $Li_2M(SO_4)_2$ (M = Fe, Co and Ni) samples. All samples dissolved in 5M HCl to form a dilute solution containing LiCl and MCl_2 (M = Mn, Co and Ni) or $FeCl_3$. The enthalpy contribution due to adsorbed water on $Li_2M(SO_4)_2 \cdot nH_2O$ samples (M = Mn, Fe, Co and Ni) were corrected ($\Delta H_{solun\text{-}corre}$) using the thermochemical cycle given in Table 2. For monoclinic $Li_2Fe(SO_4)$ phase, the XRD refinement and TGA results show the presence of $FeSO_4$ (~ 2.75 wt %) and water (~0.058 mol) and hence additional correction was done using $FeSO_4 \cdot 7H_2O$ (~ 0.027 mol) as an impurity phase. The exact hydration state of the $FeSO_4$ in the sample is not altogether clear so this correction is approximate. However its magnitude is within the experimental error of the calorimetric measurements. Finally, the enthalpies of formation of $Li_2M(SO_4)_2$ (M = Mn, Fe, Co and Ni) at 25 °C from their constituent binary sulfates, Li_2SO_4 and MSO_4 (M = Fe, Co and Mn) were calculated using

corrected enthalpies of dissolution of samples ($\Delta H_{solun\text{-}corre}$) in an appropriate thermochemical cycle (see Table 2). The formation enthalpies for monoclinic $Li_2M(SO_4)_2$ (M = Mn, Fe and Co) phases vary from 0.78 ± 0.74 to 3.51 ± 0.24 kJ/mol and that for orthorhombic $Li_2M(SO_4)_2$ (M = Fe, Co and Ni) phases from 2.34 ± 0.58 to 14.51± 0.31 kJ/mol (see Table 1). Since these materials can be synthesized from the binary sulfates under some sets of conditions, their Gibbs free energies of formation from the binary sulfates are presumably negative, implying significant positive entropies of formation. The sources of such entropy terms are discussed below.

Figure 4 shows the relative stabilities of monoclinic and orthorhombic phases in terms of dissolution and formation enthalpies of lithium metal sulfates, $Li_2M(SO_4)_2$ (M = Mn, Fe, Co and Ni) as a function of cation radius. For both monoclinic and orthorhombic phases, the dissolution enthalpy becomes less exothermic on moving from Ni to Mn with increase in cation size (Fig 4a). The enthalpies of dissolution of monoclinic phases are less exothermic compared to orthorhombic phases for Fe and Co containing $Li_2M(SO_4)_2$ samples, which suggest that the monoclinic phases are more stable than their orthorhombic counterparts. The enthalpies of formation of $Li_2M(SO_4)_2$ (M = Mn, Fe, Co and Ni) samples from lithium sulfate and metal sulfates as a function of cation radius are given in Figure 4b. For Fe and Co containing samples that exist in both polymorphic forms, the enthalpies of formation for monoclinic phases are less endothermic than their orthorhombic analogues, which show that the monoclinic phases are energetically more stable relative to the orthorhombic phases. In contrast to earlier reported energetic trends in layered hydroxysulfates,[39] the stability of both monoclinic and orthorhombic (except for Ni) $Li_2M(SO_4)_2$ (M = Mn, Fe, Co) phases increases with increase in ionic radius, which might have bearing with changes in structure and nature of bonding of sulfate groups from hydroxysulfates due to its different electronegativity.

The heats of formation of $Li_2M(SO_4)_2$ (M = Mn, Fe, Co and Ni) are found to be positive and they decrease with increase in ionic radius for both monoclinic and orthorhombic (except for Ni) phases. Among orthorhombic phases, $Li_2Ni(SO_4)_2$ does not follow this trend and shows greater thermodynamic stability, thus it is not surprising that the nickel compound was the first reported phase in this family. Such positive enthalpies of formation were also observed earlier for $LiMSO_4F$ (M = Fe, Mn) triplite and tavorite polymorphs, where configuration entropy factors from atomically disordered sites for Li and metal atoms stabilized triplite over tavorite. Sources of entropy include lattice vibrations, spin and magnetic terms, and configurational terms arising from positional disorder and defect formation [32,33]. However, no obvious configurational entropy contribution could be derived from the crystal structures of both $Li_2M(SO_4)_2$ polymorphs. Recent atomistic modeling and DFT studies by Clark et al. have revealed that the creation of vacancies and defects is energetically unfavorable in monoclinic $Li_2M(SO_4)_2$ (M = Fe, Mn, Co).[62] This prompted us look for other sources of entropy. The first is based on the feasibility of SO_4 rotational disorder as observed in many sulfate-based materials. Though the enthalpy of formation from binary sulfates is positive for both orthorhombic and monoclinic polymorphs, it is significantly larger for the orthorhombic phase. This suggests that, for the orthorhombic phase to be stable relative to the binary sulfates, it must have higher entropy as well. Measurement of the heat capacity of both phases from cryogenic to ambient temperature could constrain the entropy difference, but such measurements would be complicated by the air and water sensitivity of the materials and is beyond the scope of this work. Some qualitative insight into this entropy term comes from ionic conductivity measurements since cation migration within a structure is sensitive to disorder, with the ionic conductivity increasing with increasing disorder. We earlier reported that the ionic conductivity is greater for the orthorhombic than the monoclinic phase,[42] supporting its possible disorder and higher entropy.

The results of thermodynamic studies of $Li_2M(SO_4)_2$ (M = Mn, Fe, Co and Ni) can explain the driving force behind the phase formation, polymorphism and transformation behavior observed in these materials.[42] Orthorhombic $Li_2M(SO_4)_2$ phases (M = Fe and Co), having lower energetic stability than the corresponding monoclinic phases, are metastable at ambient conditions and hence their synthesis requires synthetic methods capable of generating large entropy via disorder such as ball milling at room temperature. The thermodynamically stable monoclinic phase forms at high temperature by ceramic methods. Consequently, the metastable orthorhombic $Li_2M(SO_4)_2$ (M = Fe, Co) polymorphs undergo irreversible phase transformation to monoclinic forms on heat treatment. Such phase transformation were observed in DSC curves as small exothermic peaks as well as in the heating experiments reported earlier by Lander et al [62]. Interestingly, orthorhombic $Li_2Ni(SO_4)_2$ that exhibits greater thermodynamic stability was formed by a ceramic route on heat treatment at 500 °C for 24 hours and does not transform into monoclinic phase on heating.

Lander et al.[42] reported the phase transformation of monoclinic $Li_2M(SO_4)_2$ (M = Fe, Co) to the orthorhombic phase on ball milling for 2 hours. Ball milling generally favors defect creation and the driving force for this phase transformation could be the energetically more unfavorable creation of vacancies and other point defects in monoclinic $Li_2M(SO_4)_2$ phases as reported earlier on the basis of DFT calculations.[62]

The stability and phase transformation among polymorphs of lithium sulfate polyanionic compounds have distinct correlation with their defect chemistry and their long and short range structures. For $LiFeSO_4F$ and $LiFeSO_4OH$,[24, 25, 28, 29] metastable tavorite polymorphs with corner shared metal polyhedra have lower symmetry than the stable high symmetry monoclinic triplite ($LiFeSO_4F$) and layered ($LiFeSO_4OH$) polymorphs having edge shared octahedra. However, the short range structure of triplite ($LiFeSO_4F$) and layered ($LiFeSO_4OH$) polymorphs have distorted metal polyhedra with

atomically disordered metal sites and lower sulfate binding symmetry.[38, 39] Hence the use of ball milling and/or SPS techniques that promotes creation of vacancies, defects and disorder, as a result increases the lattice entropy favoring triplite and layered phases, while metastable tavorite polymorphs could be formed only by soft chemical synthetic approaches.

Turning to the ball milling method, our earlier studies[6, 38, 39] predict the formation of the denser phase and this holds here as the denser orthorhombic $Li_2M(SO_4)_2$ polymorph was obtained. On the other hand, when using phase stability as an indicator, we cannot establish a trend since the less stable orthorhombic $Li_2M(SO_4)_2$ phase was obtained while the most stable polymorphs were stabilized by mechanical milling when studying polymorphism in $LiFeSO_4F$ and $LiFeSO_4OH$. So caution must be exercised before generalizing too hastily. We successfully correlated synthesis conditions, phase stability and redox potential when dealing with polymorphism of $LiFeSO_4F$ and $LiFeSO_4OH$ since the most stable and denser phase showed the greater redox potential. This trend is contradicted here since orthorhombic $Li_2Fe(SO_4)_2$ which is the denser phase shows neither the higher stability nor the same voltage. A possible reason for such complications is that thermodynamics does not require that entropy scale with volume, though it often does. Thus general trends in correlating physical and thermodynamic properties must be extrapolated with great caution to unknown systems.

4. Conclusions

. The $Li_2M(SO_4)_2$ (M = Mn, Fe, Co and Ni) polymorphs have positive enthalpies of formation from binary sulfates, and show a decrease in energetic metastability with increasing ionic radius for both monoclinic and orthorhombic (except for Ni) polymorphs. Hence the formation of these phases appears to be entropy driven due to the possible vibrational/rotational disorder of the SO_4 tetrahedra

Acknowledgements

The calorimetric studies were supported by the U.S. Department of Energy, grant DEFG0203ER46053. We thank S. Radha for her help during sample characterization and calorimetric measurements at UC Davis.

Table 1. The water content and calorimetric data of Li*M*SO_4OH (*M* = Co, Fe and Mn) samples along with *M*SO_4 (*M* = Mn, Fe, Co and Ni) and Li_2SO_4 reagents.

Composition	H_2O (n) mol	ΔH_{solun} kJ/mol	$\Delta H_{solun\text{-}corre\ H2O}$ kJ/mol	$\Delta H_{formation}$ kJ/mol	Ionic radius (Å)
Reagents					
Li_2SO_4	0.0	3.42 ± 0.06 (4)	3.42 ± 0.06		
$MnSO_4$	0.00	-21.20 ± 0.66 (5)	-21.20 ± 0.66		
$FeSO_4$	0.00	-35.44 ± 0.42 (5)	-35.44 ± 0.42		
$CoSO_4$	0.193	-37.52 ± 0.12 (5)	-37.44 ± 0.12		
$NiSO_4$	0.00	-50.08 ± 0.05 (5)	-50.08 ± 0.05		
$FeSO_4 \cdot 7\ H_2O$		47.1 ± 0.3 (4)[63]	49.9 ± 0.3		
Monoclinic samples					
$Li_2Mn(SO_4)_2$	0.029	-18.58 ± 0.34 (7)	-18.57 ± 0.34	0.78 ± 0.74	0.83
$Li_2Fe(SO_4)_2$	0.058	-31.69 ± 0.44 (7)	-33.01 ± 0.45[a]	0.99 ± 0.61	0.78
$Li_2Co(SO_4)_2$	0.00	-37.54 ± 0.2 (6)	-37.54 ± 0.2	3.51 ± 0.24	0.745
Orthorhombic samples					
$Li_2Fe(SO_4)_2$	0.117	-40.80 ± 0.40 (9)	-40.75 ± 0.40	8.73 ± 0.34	0.78
$Li_2Co(SO_4)_2$	0.099	-48.58 ± 0.28 (8)	-48.54 ± 0.28	14.51± 0.31	0.745
$Li_2Ni(SO_4)_2$	0.01	-49.00 ± 0.30 (8)	-49.00 ± 0.30	2.34 ± 0.58	0.69

n = Water adsorbed on sample exposure to air; ΔH_{solun} = enthalpy of dissolution in 5M HCl; $\Delta H_{solun\text{-}corre\ H2O}$ = enthalpy of dissolution corrected for water as physically adsorbed; $\Delta H_{formation}$ = enthalpy of formation from lithium sulfate and transition metal sulfate; [a] Also corrected for 0.027 $FeSO_4 \cdot 7\ H_2O$ impurity.

Table 2. Thermochemical cycles for adsorbed water correction ($\Delta H_{sol\text{-}corr\text{-}H2O}$) and enthalpy of formation ($\Delta H_{formation}$) of monoclinic and orthorhombic $Li_2M(SO_4)_2$ (M = Mn, Fe Co and Ni).

I - Reaction Scheme: Correction for adsorbed water ($\Delta H_{sol\text{-}corr\text{-}H2O}$)	**Enthalpy Measurement**
$Li_2M(SO_4)_2 \cdot n\ H_2O_{(s,\ 25\ ^oC\ )} + 4HCl_{(l,\ 25\ ^oC\ )} \rightarrow 2\ LiCl_{(sln,\ 25^oC)} + MCl_{2\ (sln,\ 25^oC)} + 2H_2SO_{4(sln,\ 25^oC)} + n\ H_2O_{(sln,\ 25^oC)}$	$\Delta H_1 = \Delta H_{solun}(\ Li_2M(SO_4)_2 \cdot n\ H_2O)$
$H_2O_{\ (l,\ 25^oC)} \rightarrow H_2O_{\ (sln,\ 25^oC)}$	ΔH_2 = -0.4 kJ/mol [64]
$Li_2M(SO_4)_{2\ (s,\ 25\ ^oC\ )} + 4HCl \rightarrow 2LiCl_{(sln,\ 25^oC)} + MCl_{2\ (sln,\ 25^oC)} + 2H_2SO_{4(sln,\ 25^oC)}$	$\Delta H_3 = \Delta H_{sol\text{-}corr\text{-}H2O}(\ Li_2M(SO_4)_2 = \Delta H_1 - n\ \Delta H_2$
II - Reaction Scheme: Enthalpy of formation ($\Delta H_{formation}$)	
$Li_2M(SO_4)_{2\ (s,\ 25\ ^oC)} + 4\ HCl \rightarrow 2\ LiCl_{(sln,\ 25^oC)} + MCl_{2\ (sln,\ 25^oC)} + 2\ H_2SO_{4(sln,\ 25^oC)}$	$\Delta H_3 = \Delta H_{sol\text{-}corr\text{-}H2O}\ (\ Li_2M(SO_4)_2)$
$Li_2SO_{4(s,\ 25^oC)} + 2\ HCl \rightarrow 2\ LiCl_{(sln,\ 25^oC)} + H_2SO_{4\ (sln,\ 25^oC)}$	$\Delta H_4 = \Delta H_{solun}(\ Li_2SO_4)$
$MSO_{4\ (s,\ 25^oC)} + 2\ HCl \rightarrow MCl_{2\ (sln,\ 25^oC)} + H_2SO_{4(sln,\ 25^oC)}$	$\Delta H_5 = \Delta H_{solun}(MSO_4)$
$Li_2SO_{4(s,\ 25^oC)} + MSO_{4\ (s,\ 25^oC)} \rightarrow Li_2M(SO_4)_{2\ (s,\ 25\ ^oC)}$	$\Delta H_6 = \Delta H_{formation}\ (\ Li_2M(SO_4)_2) = -\Delta H_3 + \Delta H_4 + \Delta H_5$

- Fe bearing samples form yellow solution in 5M HCl due to Fe^{3+} formation.

Figure 1. Powder XRD patterns of monoclinic (*M* = Mn, Fe and Co) and orthorhombic (*M* = Fe, Co and Ni) lithium sulfate, $Li_2M(SO_4)_2$ samples (* = $FeSO_4$).

Figure 2. Crystal structures of (a) monoclinic and (b) orthorhombic lithium sulfate $Li_2M(SO_4)_2$ structures. The blue octahedra and the yellow tetrahedra correspond to MO_6 and SO_4. The blue atoms represent Li^+ ions.

Figure 3. FTIR spectra showing the region for sulfate absorption bands in (a) monoclinic and (b) orthorhombic $Li_2M(SO_4)_2$ (*M* = Mn, Fe, Co, Ni) samples.

Figure 4. Enthalpies of (a) dissolution in 5M HCl in 25 °C and (b) formation from Li_2SO_4 and MSO_4 at 25 °C of $Li_2M(SO_4)_2$ (*M* = Mn, Fe, Co, and Ni) samples.

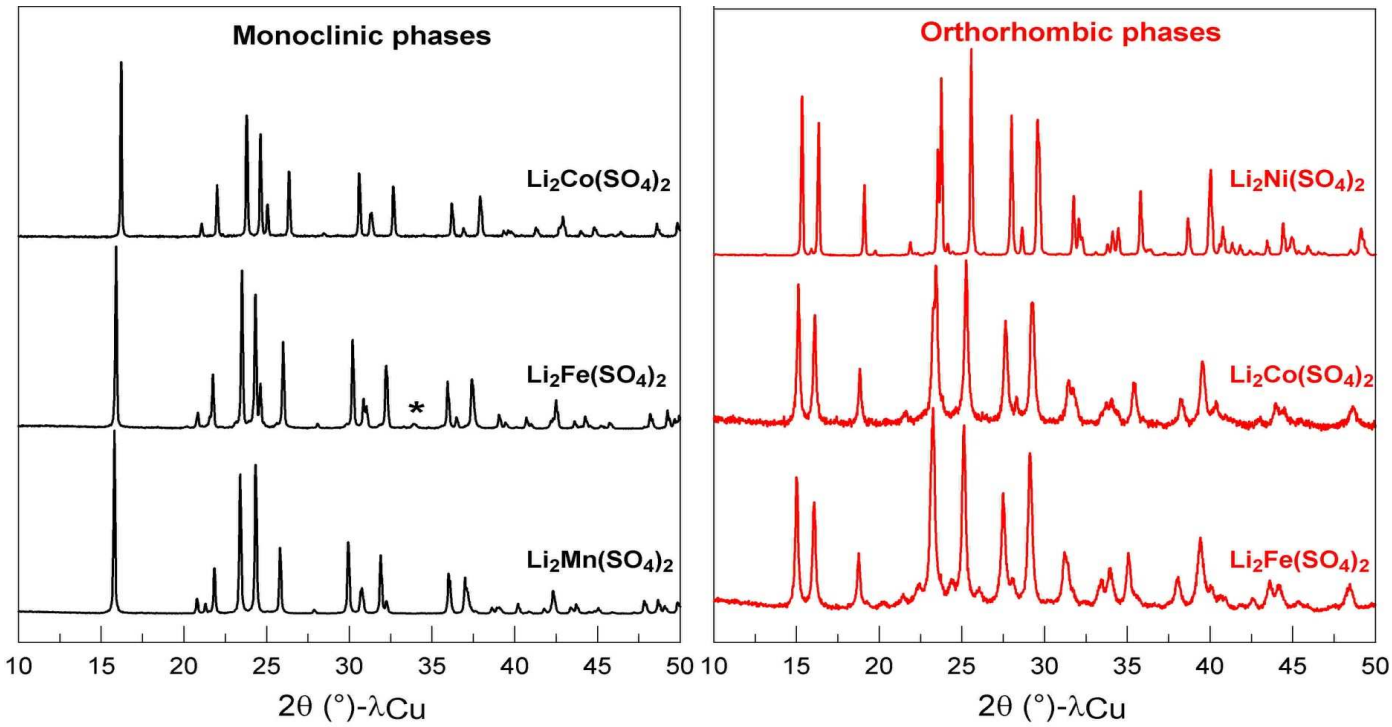
Monoclinic phases
Li2Co(SO4)2
Li2Fe(SO4)2
*
Li2Mn(SO4)2
10 15 20 25 30 35 40 45 50
2θ (°)-λCu
Orthorhombic phases
Li2Ni(SO4)2
Li2Co(SO4)2
Li2Fe(SO4)2
10 15 20 25 30 35 40 45 50
2θ (°)-λCu

Figure 1.

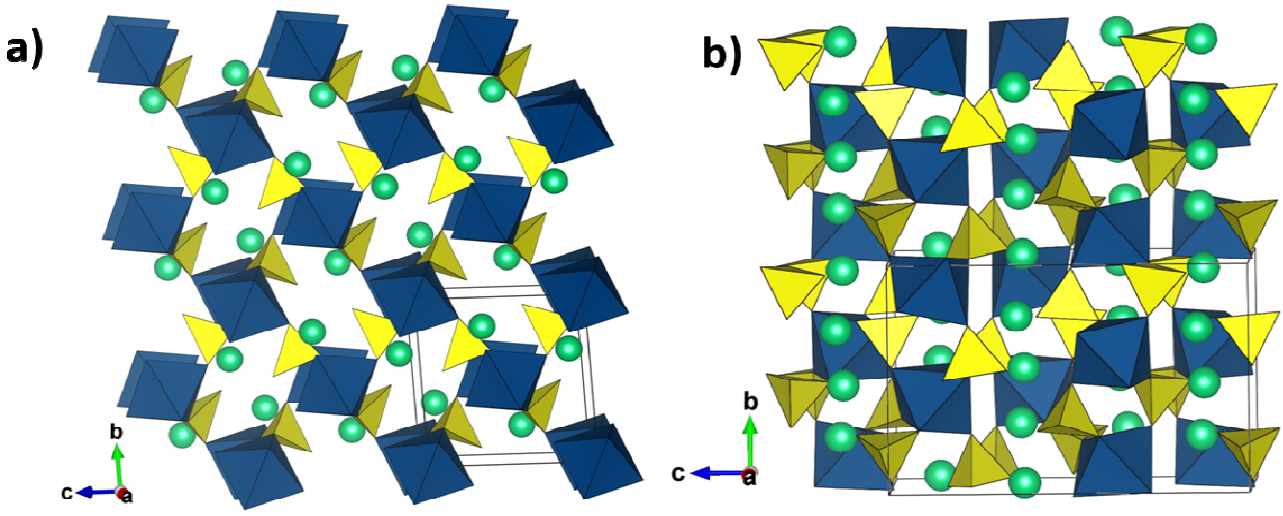

Figure 2.

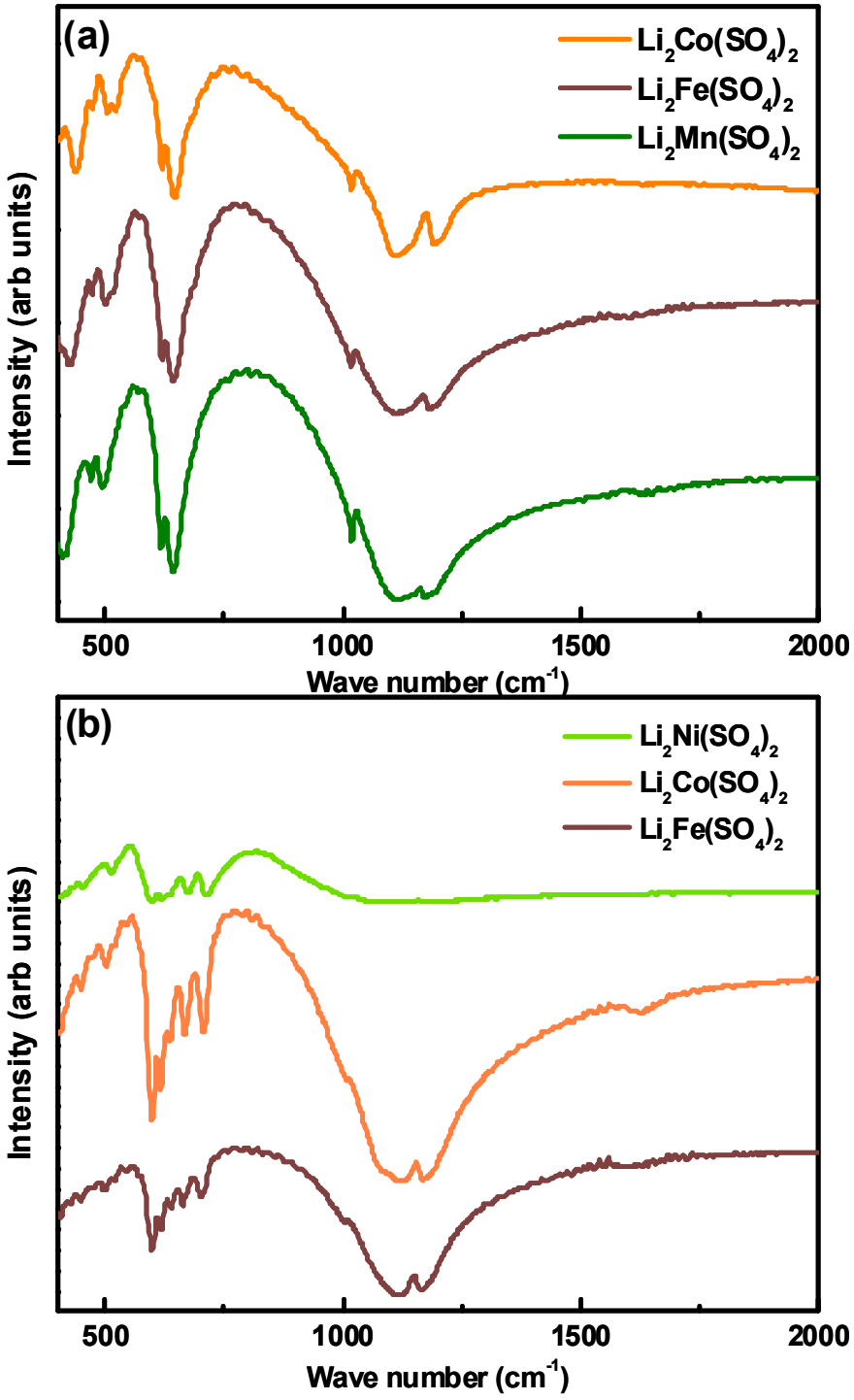
(a)
Li2Co(SO4)2
Li2Fe(SO4)2
Li2Mn(SO4)2
Intensity (arb units)
500
1000
1500
2000
Wave number (cm-1)
(b)
Li2Ni(SO4)2
Li2Co(SO4)2
Li2Fe(SO4)2
Intensity (arb units)
500
1000
1500
2000
Wave number (cm-1)

Figure 3.

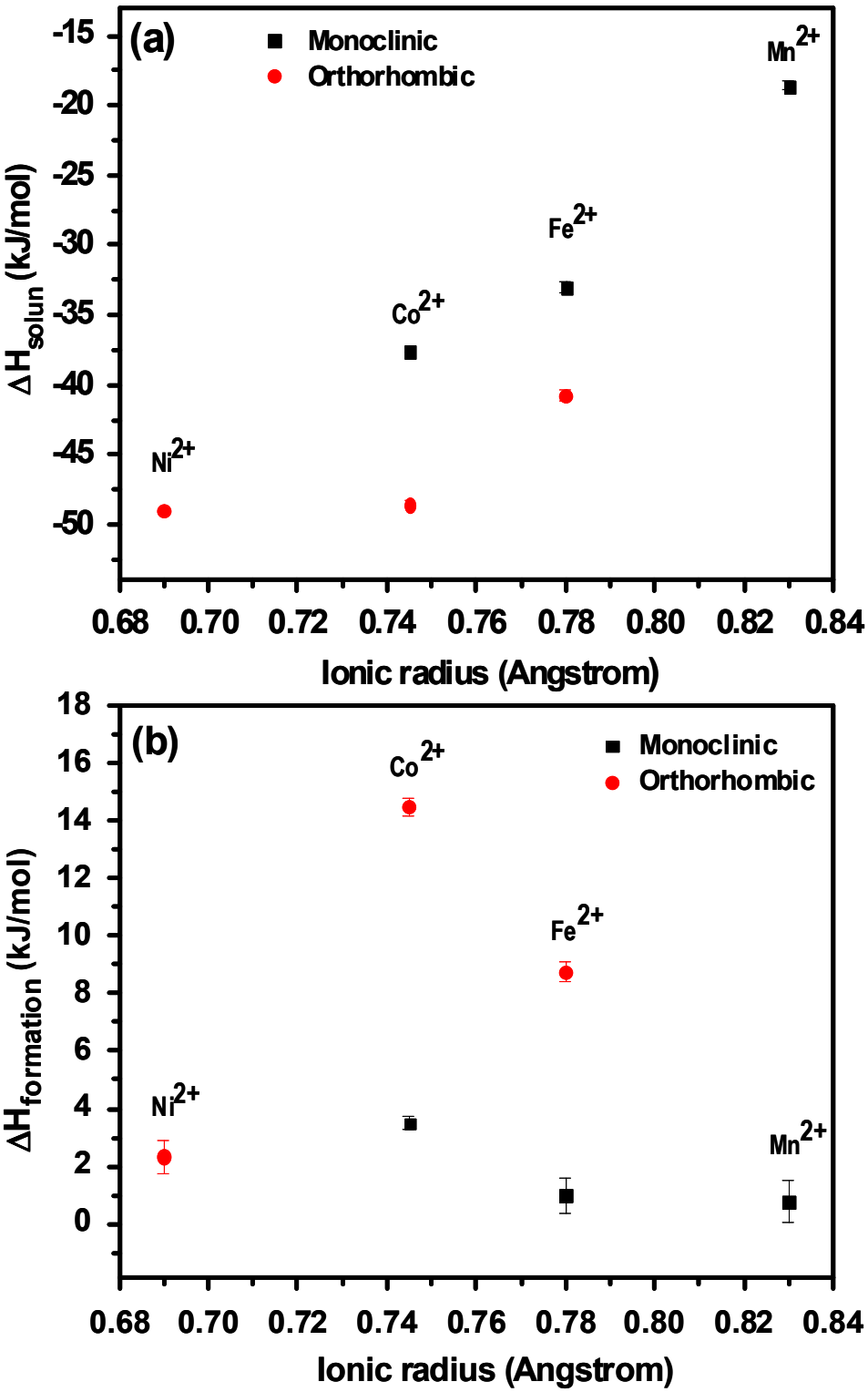
(a)
Monoclinic
Orthorhombic
Mn2+
Fe2+
Co2+
Ni2+
ΔHsolun (kJ/mol)
-15
-20
-25
-30
-35
-40
-45
-50
0.68 0.70 0.72 0.74 0.76 0.78 0.80 0.82 0.84
Ionic radius (Angstrom)
(b)
Monoclinic
Orthorhombic
Co2+
Fe2+
Ni2+
Mn2+
ΔHformation (kJ/mol)
18
16
14
12
10
8
6
4
2
0
0.68 0.70 0.72 0.74 0.76 0.78 0.80 0.82 0.84
Ionic radius (Angstrom)

Figure 4.

References

1. A. K. Padhi, V. Manivannan and J. B. Goodenough, *J. Electrochem. Soc.*, 1998, **145**, 1518-1520.
2. J. B. Goodenough, *J. Solid State Electrochem.*, 2012, **16**, 2019-2029.
3. A. S. Arico, P. Bruce, B. Scrosati, J.-M. Tarascon and W. van Schalkwijk, *Nat Mater*, 2005, **4**, 366-377.
4. V. Etacheri, R. Marom, R. Elazari, G. Salitra and D. Aurbach, *Energy & Environmental Science*, 2011, **4**, 3243-3262.
5. M. S. Islam and C. A. J. Fisher, *Chemical Society Reviews*, 2014, **43**, 185-204.
6. B. C. Melot and J. M. Tarascon, *Acc. Chem. Res.*, 2013, **46**, 1226-1238.
7. L. F. Nazar, G. Goward, F. Leroux, M. Duncan, H. Huang, T. Kerr and J. Gaubicher, *International Journal of Inorganic Materials*, 2001, **3**, 191-200.
8. M. S. Whittingham, *MRS Bulletin*, 2008, **33**, 411-419.
9. P. G. Bruce, B. Scrosati and J.-M. Tarascon, *Angewandte Chemie International Edition*, 2008, **47**, 2930-2946.
10. A. K. Padhi, K. S. Nanjundaswamy and J. B. Goodenough, *J. Electrochem. Soc.*, 1997, **144**, 1188-1194.
11. A. K. Padhi, K. S. Nanjundaswamy, C. Masquelier, S. Okada and J. B. Goodenough, *J. Electrochem. Soc.*, 1997, **144**, 1609-1613.
12. A. Yamada, S. C. Chung and K. Hinokuma, *J. Electrochem. Soc.*, 2001, **148**, A224-A229.
13. M. S. Islam, D. J. Driscoll, C. A. J. Fisher and P. R. Slater, *Chemistry of Materials*, 2005, **17**, 5085-5092.
14. P. S. Herle, B. Ellis, N. Coombs and L. F. Nazar, *Nat Mater*, 2004, **3**, 147-152.
15. P. Gibot, M. Casas-Cabanas, L. Laffont, S. Levasseur, P. Carlach, S. Hamelet, J.-M. Tarascon and C. Masquelier, *Nat Mater*, 2008, **7**, 741-747.
16. N. Recham, J. N. Chotard, J. C. Jumas, L. Laffont, M. Armand and J. M. Tarascon, *Chemistry of Materials*, 2009, **22**, 1142-1148.
17. T. N. Ramesh, K. T. Lee, B. L. Ellis and L. F. Nazar, *Electrochemical and Solid-State Letters*, 2010, **13**, A43-A47.
18. J. Barker, R. K. B. Gover, P. Burns and A. Bryan, *Electrochemical and Solid-State Letters*, 2005, **8**, A285-A287.
19. J. M. Clark, S.-i. Nishimura, A. Yamada and M. S. Islam, *Angewandte Chemie International Edition*, 2012, **51**, 13149-13153.
20. S.-i. Nishimura, M. Nakamura, R. Natsui and A. Yamada, *Journal of the American Chemical Society*, 2010, **132**, 13596-13597.
21. A. R. Armstrong, N. Kuganathan, M. S. Islam and P. G. Bruce, *Journal of the American Chemical Society*, 2011, **133**, 13031-13035.
22. M. S. Islam, R. Dominko, C. Masquelier, C. Sirisopanaporn, A. R. Armstrong and P. G. Bruce, *Journal of Materials Chemistry*, 2011, **21**, 9811-9818.
23. A. Nytén, A. Abouimrane, M. Armand, T. Gustafsson and J. O. Thomas, *Electrochem. Commun.*, 2005, **7**, 156-160.
24. P. Barpanda, M. Ati, B. C. Melot, G. Rousse, J. N. Chotard, M. L. Doublet, M. T. Sougrati, S. A. Corr, J. C. Jumas and J. M. Tarascon, *Nat. Mater.*, 2010, **10**, 772-779.
25. N. Recham, J. N. Chotard, L. Dupont, C. Delacourt, W. Walker, M. Armand and J. M. Tarascon, *Nat. Mater.*, 2010, **9**, 68-74.
26. R. Tripathi, G. R. Gardiner, M. S. Islam and L. F. Nazar, *Chemistry of Materials*, 2011, **23**, 2278-2284.
27. R. Tripathi, T. N. Ramesh, B. L. Ellis and L. F. Nazar, *Angew. Chem., Int. Ed.*, 2010, **49**, 8738-8742, S8738/8731-S8738/8739.
28. M. Anji Reddy, V. Pralong, V. Caignaert, U. V. Varadaraju and B. Raveau, *Electrochem. Commun.*, 2009, **11**, 1807-1810.

29. C. V. Subban, M. Ati, G. Rousse, A. M. Abakumov, G. Van Tendeloo, R. Janot and J.-M. Tarascon, *Journal of the American Chemical Society*, 2013, **135**, 3653-3661.
30. C. Eames, J. M. Clark, G. Rousse, J.-M. Tarascon and M. S. Islam, *Chemistry of Materials*, 2014, **26**, 3672-3678.
31. K. West, B. Zachau-Christiansen, S. Skaarup, Y. Saidi, J. Barker, I. I. Olsen, R. Pynenburg and R. Koksbang, *J. Electrochem. Soc.*, 1996, **143**, 820-825.
32. H. Y. Xu, H. Wang, Z. Q. Song, Y. W. Wang, H. Yan and M. Yoshimura, *Electrochimica Acta*, 2004, **49**, 349-353.
33. W. Xiao, J. S. Chen, C. M. Li, R. Xu and X. W. Lou, *Chemistry of Materials*, 2009, **22**, 746-754.
34. K. M. Begam, M. S. Michael, Y. H. Taufiq-Yap and S. R. S. Prabaharan, *Electrochemical and Solid-State Letters*, 2004, **7**, A242-A246.
35. K. M. Begam, M. S. Michael and S. R. S. Prabaharan, *J. Solid State Electrochem.*, 2008, **12**, 971-977.
36. Y. Janssen, D. S. Middlemiss, S.-H. Bo, C. P. Grey and P. G. Khalifah, *Journal of the American Chemical Society*, 2012, **134**, 12516-12527.
37. A. Yamada, N. Iwane, Y. Harada, S.-i. Nishimura, Y. Koyama and I. Tanaka, *Advanced Materials*, 2010, **22**, 3583-3587.
38. A. V. Radha, J. D. Furman, M. Ati, B. C. Melot, J. M. Tarascon and A. Navrotsky, *Journal of Materials Chemistry*, 2012, **22**, 24446-24452.
39. A. V. Radha, C. V. Subban, M. L. Sun, J. M. Tarascon and A. Navrotsky, *Journal of Materials Chemistry A*, 2014, **2**, 6887-6894.
40. M. Ati, M. Sathiya, S. Boulineau, M. Reynaud, A. Abakumov, G. Rousse, B. Melot, G. Van Tendeloo and J.-M. Tarascon, *Journal of the American Chemical Society*, 2012, **134**, 18380-18387.
41. M. Reynaud, M. Ati, B. C. Melot, M. T. Sougrati, G. Rousse, J.-N. Chotard and J.-M. Tarascon, *Electrochem. Commun.*, 2012, **21**, 77-80.
42. L. Lander, M. Reynaud, G. Rousse, M. T. Sougrati, C. Laberty-Robert, R. J. Messinger, M. Deschamps and J.-M. Tarascon, *Chem. Mater.*, 2014, **26**, 4178-4189.
43. M. Reynaud, M. Ati, S. Boulineau, M. T. Sougrati, B. C. Melot, G. Rousse, J. N. Chotard and J. M. Tarascon, *ECS Trans.*, 2013, **50**, 11-19, 10 pp.
44. M. Reynaud, J. Rodriguez-Carvajal, J.-N. Chotard, J.-M. Tarascon and G. Rousse, *Phys. Rev. B: Condens. Matter Mater. Phys.*, 2014, **89**, 104419/104411-104419/104419.
45. M. Reynaud, G. Rousse, J.-N. Chotard, J. Rodríguez-Carvajal and J.-M. Tarascon, *Inorganic Chemistry*, 2013, **52**, 10456-10466.
46. N. Kosova, E. Devyatkina, A. Slobodyuk and A. Gutakovskii, *J. Solid State Electrochem.*, 2014, **18**, 1389-1399.
47. N. V. Kosova and E. T. Devyatkina, *Russ J Electrochem*, 2012, **48**, 320-329.
48. N. V. Kosova, E. T. Devyatkina, A. B. Slobodyuk and S. A. Petrov, *Electrochimica Acta*, 2012, **59**, 404-411.
49. J. Isasi, S. Jaulmes, A. Elfakir and M. Quarton, *Z. Kristallogr. - New Cryst. Struct.*, 2001, **216**, 331-332.
50. K. Nakamoto, *Infrared and Raman Spectra of Inorganic and Coordination Compounds. 3rd Ed*, John Wiley and Sons, 1978.
51. H. H. Adler and P. F. Kerr, *Am. Mineral.*, 1965, **50**, 132-147.
52. M. D. Lane, *Am. Mineral.*, 2007, **92**, 1-18.
53. S. J. Hug, *Journal of Colloid and Interface Science*, 1997, **188**, 415-422.
54. A. Lunden, A. Bengtzelius, R. Kaber, L. Nilsson, K. Schroeder and R. Taerneberg, *Solid State Ionics*, 1983, **9-10**, 89-94.
55. A. Lunden, *Solid State Ionics*, 1988, **28-30**, 163-167.
56. A. Lunden, *Solid State Commun.*, 1988, **65**, 1237-1240.
57. M. Touboul, N. Sephar and M. Quarton, *Solid State Ionics*, 1990, **38**, 225-229.
58. V. V. Boldyrev, *Thermochimica Acta*, 2006, **443**, 1-36.

59. R. Aronsson, H. E. G. Knape, A. Lunden, L. Nilsson, L. M. Torell, N. H. Andersen and J. K. Kjems, *Radiation Effects and Defects in Solids*, 1983, **75**, 79-84.
60. D. Wilmer, H. Feldmann and E. Lechner Ruep, in *Zeitschrift für Physikalische Chemie/International journal of research in physical chemistry and chemical physics*, 2004, p. 1439.
61. M. Zhang, A. Putnis and E. K. H. Salje, *Solid State Ionics*, 2006, **177**, 37-43.
62. J. M. Clark, C. Eames, M. Reynaud, G. Rousse, J.-N. Chotard, J.-M. Tarascon and M. S. Islam, *Journal of Materials Chemistry A*, 2014, **2**, 7446-7453.
63. L. Mazeina, A. Navrotsky and D. Dyar, *Geochimica et Cosmochimica Acta*, 2008, **72**, 1143-1153.
64. V. B. Parker, in *National Standard Reference Data Series*, National Bureau of Standards, 1965, p. 66.